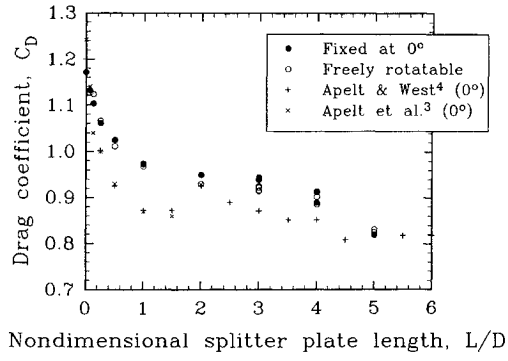

Fig. 2 Averaged drag coefficient of circular cylinder with splitter plates of various lengths: filled symbols, splitter plate fixed at 0 deg and open symbols, splitter plate free to rotate (size of symbol represents approximate accuracy of measurement; multiple data points at same *L/D* are for runs on different days).

whether the splitter plate was fixed at 0-deg angle of attack or free to rotate. In both cases, C_D decreased rapidly up to $L/D = 1$, leveled off around $2 < L/D < 3$, and then decreased slowly at higher L/D.

Discussion

For the first time, drag measurements have been obtained on a freely rotatable cylinder/splitter-plate body. It has been shown that the splitter plate reduced the drag significantly, with drag reduction increasing with splitter-plate length, just as in the case of a nonrotatable cylinder with splitter plate attached at 0 deg. In fact, there was very little difference between the drag on the cylinder with splitter plate attached at 0-deg angle of attack, and that on the cylinder/splitter-plate body free to rotate. This is consistent with the wake measurements and flow visualizations of Cimbala and Garg,[6] who reported that splitter plates larger than about 2 cylinder diameters had nearly the same effect on the wake of the cylinder regardless of whether rigidly attached or free to rotate.

For the bare-cylinder case (no splitter plate), our measured C_D is about 1.17, lower than the 1.24 reported by Apelt et al.[3] Both of these are somewhat high compared to that reported by Schlichting[10] in this Reynolds number range, i.e., around 1.12 for a smooth bare cylinder. With the addition of splitter plates, however, the present data are consistently higher than those of Apelt and co-workers.[3,4] There is also a dip in their drag coefficient between $0.5 < L/D < 2$, which did not appear in the present data, although C_D did tend to level off somewhat in this L/D range. The reasons for these discrepancies are discussed now. Model blockage in the wind tunnel was about 6% for the present experiments, the same as that of the water-tunnel experiments of Apelt and co-workers,[3,4] and neither set of data was corrected for blockage. The aspect ratio of the model used by Apelt et al.[3] was 20.6, whereas the total aspect ratio of the present model was 16. Thus, neither tunnel blockage nor aspect ratio should have played a significant role in the differences between the two experiments. The discrepancies in the two sets of data may be because Apelt et al.[3] calculated drag solely from pressure measurements on the body, whereas total drag (both pressure drag and skin friction drag) were measured in the present experiments. White[11] shows that for a bare circular cylinder, skin friction drag accounts for only about 3% of the total drag. This is not enough to bring the data of Apelt et al.[3] up to the level of the present experiments. However, additional skin friction drag would be caused by the splitter plate itself, and this was not accounted for by either Apelt et al.[3] or Apelt and West.[4]

Conclusion

In summary, for engineering applications where it is desirable to reduce the drag on a cylinder, but where the freestream flow direction is not fixed, or not known a priori, a freely rotatable splitter plate can provide nearly the same drag reduction as can a fixed splitter plate, even though it migrates to an angle not in line with the flow. A freely rotatable splitter plate, mounted to a cylinder, therefore has potential as an omnidirectional drag-reducing device.

References

[1]Roshko, A., "On the Development of Turbulent Wakes from Vortex Streets," NACA TN 2913, March 1953.

[2]Bearman, P. W., "Investigation of the Flow Behind a Two-Dimensional Model with a Blunt Trailing Edge and Fitted with Splitter Plates," *Journal of Fluid Mechanics*, Vol. 21, Pt. 2, 1965, pp. 241–255.

[3]Apelt, C. J., West, G. S., and Szewczyk, A. A., "Effects of Wake Splitter Plates on the Flow Past a Circular Cylinder in the Range $10^4 < R < 5 \times 10^4$," *Journal of Fluid Mechanics*, Vol. 61, Pt. 1, 1973, pp. 187–198.

[4]Apelt, C. J., and West, G. S., "Effects of Wake Splitter Plates on Bluff-Body Flow in the Range $10^4 < R < 5 \times 10^4$, Part 2," *Journal of Fluid Mechanics*, Vol. 71, Pt. 1, 1975, pp. 145–160.

[5]Cimbala, J. M., Garg, S., and Park, W.-J., "Effect of a Non-Rigidly-Mounted Splitter Plate on the Flow over a Circular Cylinder," *Bulletin of the American Physical Society*, Vol. 33, No. 10, 1988, p. 2249.

[6]Cimbala, J. M., and Garg, S., "Flow in the Wake of a Freely Rotatable Cylinder with Splitter Plate," *AIAA Journal*, Vol. 29, No. 6, 1991, pp. 1001–1003.

[7]Xu, J. C., Sen, M., and Gad-el-Hak, M., "Low-Reynolds Number Flow over a Rotatable Cylinder-Splitter Plate Body," *Physics of Fluids*, Vol. 2, No. 11, 1990, pp. 1925–1927.

[8]Xu, J. C., Sen, M., and Gad-el-Hak, M., "Dynamics of a Rotatable Cylinder with Splitter Plate in Uniform Flow," *Journal of Fluids and Structures*, Vol. 7, No. 4, 1993, pp. 401–416.

[9]Cimbala, J. M., and Chen, K. T., "Supercritical Reynolds Number Experiments on a Freely Rotatable Cylinder/Splitter Plate Body," *Physics of Fluids*, Vol. 6, No. 7, 1994, pp. 2440–2445.

[10]Schlichting, H., *Boundary-Layer Theory*, 7th ed., McGraw–Hill, New York, 1979, p. 17.

[11]White, F. M., *Fluid Mechanics*, 3rd ed., McGraw–Hill, New York, 1994, p. 413.

Interactions of a Vortex with an Oscillating Leading Edge

R. W. Jefferies* and D. Rockwell†
Lehigh University,
Bethlehem, Pennsylvania 18015-3085

Introduction

IMPINGEMENT of coherent vortical structures upon airfoils and blades occurs in a variety of flow configurations, including wings and tails of aircraft and blades of turbomachinery, helicopters, and wind turbines.

When a vortex interacts with a surface, it induces pressure fluctuations, which serve as the origin of unsteady loading and noise generation. The unsteady loads may be of the same order as, or even surpass, steady loads and can lead to early failure of an airfoil or blade. The associated noise generation often exceeds design limits and severely threatens system operation. Moreover, the overall system performance, based on steady-state criteria, is often degraded. An understanding of the flow physics of these vortex–surface interactions is therefore crucial.

The theoretical study of Rogler[1] and the experimental investigations of Gursul and Rockwell,[2] Kaykayoglu and Rockwell,[3] and Booth[4] show that the magnitude of the pressure fluctuation $\tilde{p}$ due to vortex interactions is greatest at the leading edge of the surface. Rogler,[1] Gursul and Rockwell,[2] Kaykayoglu and Rockwell,[3] and Wilder[5] indicate that the nature of the incident vortex, namely scale λ and circulation Γ, as well as its transverse offset δ from the leading edge, strongly influence $\tilde{p}$. Ziada and Rockwell,[6] Kaykayoglu

Received Nov. 20, 1995; revision received July 2, 1996; accepted for publication July 23, 1996; also published in *AIAA Journal on Disc*, Volume 2, Number 1.

*Ph.D. Candidate, Department of Mechanical Engineering and Mechanics; currently Captain, U.S. Air Force, Eglin Air Force Base, FL 32542.

†Paul B. Reinhold Professor, Department of Mechanical Engineering and Mechanics. Member AIAA.

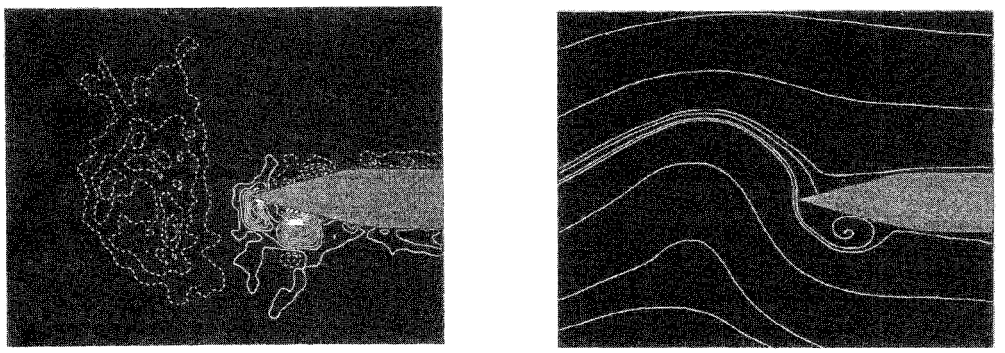

a) Stationary leading edge at an angle of attack $\alpha = 0$ deg

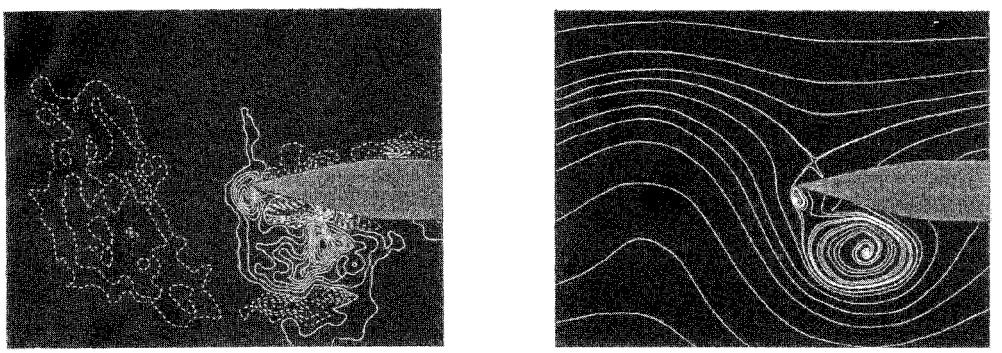

b) Oscillating leading edge at $\alpha \cong 0$ deg during its upstroke in phase ($\phi = 0$ deg) with the upstream airfoil

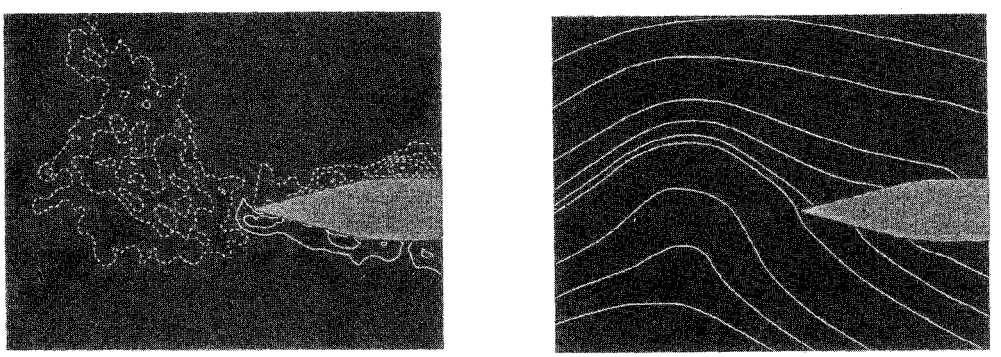

c) Oscillating leading edge at $\alpha \cong 0$ deg during its downstroke, corresponding to out-of-phase ($\phi = 180$ deg) motion of the upstream airfoil

Fig. 1 Instantaneous vorticity distributions (left column) and streamline patterns (right column). Contours of positive vorticity, corresponding to counterclockwise rotation, are denoted as solid lines, whereas negative vorticity is represented by dashed lines. The minimum contour level is $|\omega_{min}| = 10\ s^{-1}$; incremental contour levels are for negative vorticity, $\Delta\omega = 20\ s^{-1}$, and for positive vorticity, $\Delta\omega = 40\ s^{-1}$.

and Rockwell,[3] Nakagawa,[7] and Wilder[5] observed secondary vortex formation and shedding during vortex–edge interactions; Kaykayoglu and Rockwell[3] and Wilder[5] found $\tilde{p}$ to be greatest during secondary vortex shedding. Furthermore, Ziada and Rockwell[6] found the amplitude of the induced force on the leading edge depends strongly on secondary vortex shedding. These results suggest that generation of a secondary vortex strongly correlates with the induced force on the edge. In fact, generation of a secondary vortex is an inherent feature of vortex–surface interaction, even when the surface is of infinite extent, as assessed by Doligalski et al.[8] and Smith et al.[9]

The foregoing investigations have focused on stationary surfaces or edges. Relatively little is understood of the effects of controlled oscillation of an edge. Kaykayoglu,[10] using qualitative visualization, showed that a variety of vortex patterns can be generated in a mixing layer–edge system. Staubli and Rockwell[11] relate qualitative dye visualization of a jet-oscillating edge interaction to large variations of the magnitude and phase of the surface pressure on the edge.

A major, unclarified issue that emerges from all of the foregoing investigations is the degree to which the generation of vorticity concentrations from a perturbed edge can be altered by controlling the phase shift between an incident vortex and the edge motion. This study addresses the detailed structure of the interaction of an incident vortex with a leading edge that is oscillating at the frequency of the incident vortex street. Instantaneous streamline patterns and vorticity distributions allow characterization of the mechanisms of interaction as a function of the timing, or phase shift, of the incident vortex relative to the motion of the edge.

Experimental System and Techniques

Experiments were conducted in a recirculating, free-surface water channel. The transparent Plexiglas® test section had a cross section of 597 × 933 mm and a length of 4000 mm. The nominal water depth was maintained at 540 mm.

A NACA 0012 airfoil having a chord of 76 mm generated the incident vortex system. It was located upstream of a tapered flat

plate having a chord of 152 mm. Both the airfoil and plate were oriented horizontally in the channel at a depth of 260 mm beneath the free surface. A freestream speed of $U = 152$ mm/s yielded a Reynolds number $Re = 2.6 \times 10^4$, based on the flat plate chord C. The upstream airfoil was oscillated about its leading edge at a reduced frequency $k = \omega C/2U = 5$ and generated a phase-locked vortex street that convected downstream and impinged upon the leading edge of the flat plate, which also oscillated at reduced frequency $k = 5$ and amplitude of ± 5 deg. Using this approach, it was possible to maintain a defined phase shift ϕ between the oscillating airfoil and the plate, which corresponded to a prescribed time of arrival of the incident vortex, relative to the motion of the leading edge of the plate.

A laser-scanning version of high-image-density particle image velocimetry was used to obtain the instantaneous velocity field over an entire plane intersecting the leading edge of the plate. Instantaneous vorticity distributions and streamline patterns could then be calculated. A full description of this experimental approach is given by Rockwell et al.[12,13] and Rockwell and Lin.[14] The laser-scanning system employs a 4-W argon-ion laser beam that is deflected by a rotating, 72-facet mirror, producing a scanning laser sheet that illuminates seeding particles in the flow. These particles are silver-coated, hollow glass spheres with an average diameter of 14 μ and density of 1.65 g/cm^3. The flowfield illuminated by the laser sheet is captured on high-resolution 35-mm Kodak TMAX 400 film by a Nikon F4 camera with a 2X teleconverter and Micro 105-mm telephoto lens combination. The lens system has a magnification factor $M = 1{:}1.5$. Directional ambiguity is avoided by employing a bias mirror immediately in front of the camera lens. The 35-mm film negatives are digitized at a resolution of 125 pixel/mm and then interrogated using a window size of 100×100 pixels (0.8×0.8 mm) in which a single-frame, cross correlation within each window is performed. The interrogation continues for the entire image by overlapping the windows 50% and produces a vector field with a grid spacing of 0.6 mm in the plane of the laser sheet. The estimated uncertainties of the velocity and vorticity are within 0.5 and 4%, respectively.

Results

Figure 1 shows instantaneous vorticity distributions and corresponding streamline patterns for the stationary leading edge at an angle of attack $\alpha = 0$ deg (Fig. 1a) and for the oscillating leading edge at $\alpha \approx 0$ deg during its upstroke (Fig. 1b), in phase ($\phi = 0$ deg) with the upstream airfoil, and during its downstroke (Fig. 1c), corresponding to out-of-phase ($\phi = 180$ deg) motion of the airfoil.

In all cases, a large-scale vortex of negative (clockwise) vorticity (dashed lines) is incident upon the leading edge. It occurs at approximately the same position in Figs. 1a–1c. The circulation of the incident vortex is defined as $\Gamma^* = \Gamma/\pi U\lambda$, in which U is the freestream velocity and λ is the wavelength of the incident vortex street. The circulation was determined by performing the classical line integral about the contour defined by the lowest level of vorticity. For cases in Figs. 1a, 1b, and 1c, $\Gamma^* = -0.082$, -0.081, and -0.081, respectively.

For the stationary edge (Fig. 1a), both a secondary vortex of positive vorticity (solid lines) and a tertiary vortex of negative vorticity are evident along the lower surface. These vortices have values of $\Gamma^* = 0.057$ and -0.003, respectively. The streamline pattern corresponding to the secondary vortex exhibits inward-spiraling streamlines, i.e., a stable focus.

For the oscillating edge, at $\phi = 0$ deg (Fig. 1b), both a secondary and tertiary vortex are visible on the lower surface of the edge in the vorticity plots. Relative to the stationary edge of Fig. 1a, they have a much larger scale, suggesting that their values of circulation are substantially larger than those of Fig. 1a. In fact, the values of Γ^* for the secondary and tertiary vortices are 0.142 and -0.027; these values therefore exceed the corresponding ones from the stationary edge by factors of approximately 2.5 and 9.0. The small-scale secondary vortex initially shed from the tip of the edge in Fig. 1b is severed from the major secondary vortex by formation of the tertiary vortex. The streamline patterns also reveal these features of the secondary vortex/tertiary vortex interaction. Both the small-scale and major secondary vortices exhibit outward-spiraling streamlines corresponding to an unstable focus.

When $\phi = 180$ deg, corresponding to Fig. 1c, the vorticity has a relatively low level and is distributed nearly symmetrically along the upper and lower surfaces of the edge. Neither secondary nor tertiary vortices are formed, confirmed by the corresponding streamline patterns.

Conclusions

Oscillations of a leading edge, involving a controlled phase shift between the incident vortex and the edge motion, can dramatically alter the patterns of vortices in the vicinity of the leading edge. The degree of phase shift influences the development of secondary and tertiary vortices from the tip of the edge, and proper choice of this shift can actually preclude their generation. The original investigation of this interaction showed that formation of a secondary vortex was coincident with larger magnitudes of induced force on the leading edge. Its elimination may therefore significantly alter the magnitude of the loading on the edge. This observation suggests the phase of the leading-edge oscillation can potentially be used as a means of controlling vortex–blade interactions.

Acknowledgments

The authors gratefully acknowledge the financial support of U.S. Air Force Office of Scientific Research Grant F49620-93-1-0075 and National Science Foundation Grant CTS-9422432, and the expertise provided by Emerson Wagner and Frank Klucsik in fabricating the experimental apparatus.

References

[1]Rogler, H., "The Interaction Between Vortex-Array Representations of Free-Stream Turbulence and Semi-Infinite Flat Plates," *Journal of Fluid Mechanics*, Vol. 87, 1978, pp. 583–606.

[2]Gursul, I., and Rockwell, D., "Vortex Street Impinging upon an Elliptical Leading Edge," *Journal of Fluid Mechanics*, Vol. 211, 1990, pp. 211–242.

[3]Kaykayoglu, R., and Rockwell, D., "Vortices Incident upon a Leading Edge: Instantaneous Pressure Fields," *Journal of Fluid Mechanics*, Vol. 156, 1985, pp. 439–461.

[4]Booth, E. R., "Experimental Observations of Two-Dimensional Blade-Vortex Interaction," *AIAA Journal*, Vol. 28, No. 8, 1990, pp. 1353–1359.

[5]Wilder, M. C., "Airfoil-Vortex Interaction and the Wake of an Oscillating Airfoil," Ph.D. Dissertation, Virginia Polytechnic Inst. and State Univ., Blacksburg, VA, 1992.

[6]Ziada, S., and Rockwell, D., "Vortex-Leading-Edge Interaction," *Journal of Fluid Mechanics*, Vol. 118, 1982, pp. 79–107.

[7]Nakagawa, T., "On Unsteady Airfoil-Vortex Interaction," *Acta Mechanica*, Vol. 75, 1988, pp. 1–13.

[8]Doligalski, T. L., Smith, C. R., and Walker, J. D. A., "Vortex Interactions with Walls," *Annual Review of Fluid Mechanics*, Vol. 26, 1994, pp. 537–616.

[9]Smith, C. R., Walker, J. D. A., Haidari, A. H., and Sobrun, U., "On the Dynamics of Near-Wall Turbulence," *Philosophical Transactions of the Royal Society of London, Series A: Mathematical and Physical Sciences*, Vol. 336, 1991, pp. 131–175.

[10]Kaykayoglu, C. R., "Active Control of a Mixing Layer by Upstream Influence from an Oscillating Edge," *Journal of Fluids and Structures*, Vol. 3, 1989, pp. 1–16.

[11]Staubli, T., and Rockwell, D., "Interaction of an Unstable Planar Jet with an Oscillating Leading-Edge," *Journal of Fluid Mechanics*, Vol. 176, 1987, pp. 135–167.

[12]Rockwell, D., Towfighi, J., Magness, C., Akin, O., Corcoran, T., Robinson, O., and Gu, W., "Instantaneous Structure of Unsteady Separated Flows via Particle Image Velocimetry," Fluid Mechanics Labs., Dept. of Mechanical Engineering and Mechanics, Lehigh Univ., Rept. PI-1, Bethlehem, PA, Feb. 1992.

[13]Rockwell, D., Magness, C., Towfighi, J., Akin, O., and Corcoran, T., "High-Image-Density Particle Image Velocimetry Using Laser Scanning Techniques," *Experiments in Fluids*, Vol. 14, 1993, pp. 181–192.

[14]Rockwell, D., and Lin, J.-C., "Quantitative Interpretation of Complex, Unsteady Flows via High-Image-Density Particle Image Velocimetry," *Optical Diagnostics in Fluid and Thermal Flow*, Proceedings of SPIE—The International Society for Optical Engineering, Vol. 2004, 1993, pp. 490–503.